NASA Technical Memorandum 87110

Creep-Fatigue Behavior of NiCoCrAlY Coated PWA 1480 Superalloy Single Crystals

Robert V. Miner, John Gayda,
and Mohan G. Hebsur
Lewis Research Center
Cleveland, Ohio

Prepared for the
Symposium on Low-Cycle Fatigue Directions for the Future
sponsored by the American Society for Testing and Materials
Bolton Landing, New York, September 30—October 4, 1985

NASA

CREEP-FATIGUE BEHAVIOR OF NiCoCrAlY COATED PWA 1480 SUPERALLOY SINGLE CRYSTALS

Robert V. Miner, John Gayda, and Mohan G. Hebsur*
National Aeronautics and Space Administration
Lewis Research Center
Cleveland, Ohio 44135

SUMMARY

Single crystal specimens of a Ni-base superalloy, PWA 1480, with a low pressure plasma sprayed NiCoCrAlY coating were tested in various 0.1 Hz fatigue and creep-fatigue cycles both at 1015 and 1050 °C. Creep-fatigue tests of the cp, pc, and cc types were conducted with various constant total strain ranges employing creep dwells at various constant stresses. Considerable cyclic softening occurred as was evidenced particularly by rapidly increasing creep rates in the creep-fatigue tests. The cycle time in the creep-fatigue tests typically decreased by more than 80 percent at 0.5 N_f.

Though cyclic life did correlate with $\Delta\varepsilon_{in}$, a better correlation existed with $\Delta\sigma$ for both the fatigue and creep-fatigue tests, and poor correlations were observed with either σ_{max} or the average cycle time. A model containing both $\Delta\sigma$ and $\Delta\varepsilon_{in}$, $N_f = \alpha\, \Delta\varepsilon_{in}^{\beta}\, \Delta\sigma^{\gamma}$, with best fit values of α for each cycle type, but the same values of β and γ, was found to provide good correlations. Life lines were not greatly different among the cycle types, differing only by a factor of about three. The cp cycle life line was lowest for both test temperatures, however among the other three cycle types there was no consistent ranking. For all test types failure occurred predominately by multiple internal cracking originating at pores. The strong correlation of life with $\Delta\sigma$ may reflect a significant crack growth period in the life of the specimens. The lack of improvement in the models when average cycle time was considered reflects that neither is there a large effect of strain rate on the damage mechanisms in the single crystal material, nor any environmental effect due to the internal cracking mode of failure.

INTRODUCTION

Nickel-base superalloy single crystals with protective metallic coatings are employed as blades and vanes in aircraft gas turbine engines. Thermomechanical fatigue is a major life limiting factor in these components. The present study of high temperature fatigue and creep-fatigue behavior is part of a program to identify the basic features of the effects of temperature, creep, fatigue, and environment on the behavior of a single crystal superalloy, a bulk coating alloy, and the coated alloy system. The goal is to test the feasibility of a life prediction model for coated single crystal specimens in laboratory thermomechanical test cycles based on the individual behaviors of the superalloy and coating, and mechanical and thermal analyses of the coated specimen. The framework of such a model might be extended to predict the life of actual components.

*NRC-NASA Research Associate.

To provide the best opportunity for success, it was decided to model a specific superalloy-coating system, and to select one which has had considerable commercial production experience: the Ni-base superalloy, PWA 1480, and the NiCoCrAlY coating, PWA 276, inventions of the Pratt and Whitney Aircraft Company of the United Technologies Corporation. This coating has the additional benefit of being low pressure plasma sprayed. It may be deposited in thicknesses great enough for the preparation of mechanical test specimens.

Isothermal behavior has been studied first, since it was desired to base any thermomechanical fatigue model on more simple isothermal data if possible. Also, it was not clear what to expect of the creep-fatigue behavior of a superalloy without grain boundaries. For instance, the common creep damage mechanisms of grain boundary cavitation or sliding were certain not to occur.

A series of fatigue and creep-fatigue tests of the types commonly designated as pp, cp, pc, and cc were conducted. The letters p and c refer to rapid "plastic" and slow "creep" type deformation, and the first and second letters to the tensile and compressive portions of the cycle, respectively. These tests were conducted at various constant total strain ranges. The creep-fatigue cycles employed constant stress dwells at the maximum and/or minimum load.

After the first series of tests it was discovered that they had been conducted at 1015 °C, rather than at 1050 °C as intended. Also, it appeared that the dwell stress level effected life in the creep-fatigue cycles, but the result was somewhat confounded since the controlled dwell stresses and total strain ranges had been varied commensurately in order to minimize test times. In a second series of tests, conducted at 1050 °C, total strain range and dwell stress level were varied as independently as practicable. It will be seen that both series of tests indicate an important effect of stress on the cyclic life of the coated superalloy single crystals.

Discussion will center on the constitutive behavior, life behavior, and failure modes for the individual cycle types. It will be shown that creep does not greatly influence the fatigue life of this material, or at least it is difficult to introduce creep damage using stress dwells. Probably because of this, a single life relation provides a fairly good correlation for all the cycle types investigated, though it is rather unconventional in being based on $\Delta\varepsilon_{in}$ and $\Delta\sigma$, and thus more sophisticated damage interaction models have not been investigated. A thorough set of data from the 44 tests conducted is included herein so that those wishing to corroborate generalizations made or try their own analysis may do so.

MATERIALS AND PROCEDURES

Materials

The single crystal superalloy studied herein is designated PWA 1480 and was developed by Pratt and Whitney Aircraft for application as aircraft gas turbine blades and vanes (ref. 1). The alloy has the following nominal composition: 10Cr, 5Al, 1.5Ti, 12Ta, 4W, 5Co, balance Ni, in weight percent. This alloy contains about 65 vol % of the γ' phase, but essentially no carbides or

borides, since C, B, and Zr are not necessary for grain boundary strengthening in single crystals. The single crystal specimens were grown as round bars about 21 mm in diameter and 140 mm long.

The bars were solution treated for 4 hr at 1290 °C. This was done before machining since it could lead to recrystallization after machining. Bars having their <001> within less than 7° of the axis were selected for the LCF specimens. After machining, the LCF specimens were coated with a NiCoCrAlY alloy by low pressure plasma spraying. The PWA 276 coating composition was 20Co, 17Cr, 12.4Al, 0.5Y, and balance Ni, all in weight percentage. The coating thickness was about 0.12 mm. After coating, the specimens were given a diffusion treatment of 1080 °C for 4 hr and then aged a 870 °C for 32 hr.

Interdendritic porosity is known to be a problem in single crystal superalloys, and those studied herein were no exception. The crystals tested contained an average of about 0.3 vol % of porosity. The pore diameter averaged about 7 μm with a standard deviation of about 6 μm. The yield strengths of these crystals averaged about 10 percent lower from room temperature to 1050 °C than those of the crystals studied by Shah and Duhl (ref. 2). A larger fraction of large γ' particles in the crystals studied herein indicated that the solution treatment temperature was actually lower than expected.

Test Procedures

The testing facility used in this investigation has been described elsewhere (ref. 3) except for the computer control facility used for the later tests, and thus will be described only briefly herein. Fatigue tests at 0.1 Hz and creep-fatigue tests were conducted using an hourglass type specimen and diametral strain control. The nominal diameters of the single crystal specimens before and after coating were 6.35 and 6.60 mm, respectively. Heating was produced by the passage of alternating current directly through the specimen. A thermocouple for temperature control was attached to the specimen about 5 mm from the minimum section. The control temperature was adjusted to give the desired temperature at the minimum diameter as measured by an optical pyrometer.

Diametral strain control of the Ni-base superalloy single crystals does not present a problem since cubic crystals are elastically isotropic in the plane normal to a <001> crystal axis. As stated previously, all specimens had their axis within 7° of the <001> crystallographic direction. Further, at the test temperatures employed, inelastic deformation in this material also appeared homogeneous and isotropic. Still, care was taken to place the extensometer across one of the <001> nearly perpendicular to the specimen axis to guard against effects of small deviations of the specimen axis from the <001>.

It had been intended to conduct tests only at 1050 °C, however when a laboratory renovation provided new computer control, some additional tests were conducted. It was found during these additional tests that the optical pyrometer had been out of calibration during the previous testing. What had been intended as 1050 °C tests were actually conducted at about 1015 °C. Both because there was some uncertainty about the temperature of the first tests, and because it was becoming suspected that life in the creep-fatigue cycles was influenced by the dwell stress level, a set of computer controlled tests were conducted at 1050 °C. In these tests, total strain range and dwell stress

level were varied as independently as practicable. It will be seen, however, that life behavior in the lower temperature tests shows the same dependencies on strain and stress stress as in the 1050 °C tests even though the two "independent" variables are more highly correlated.

All tests were controlled at constant total diametral strain range. In the creep-fatigue cycles, constant stress dwells were employed. In the first set of tests, those at 1015 °C, the dwell stress limits were controlled using an electromechanical programmer. In the 1050 °C tests, a Data General S/20 computer was employed to control the dwell stress limits.

The frequency of the pp tests at both temperatures was about 0.1 Hz. The creep-fatigue tests employed about the same ramp rates as the pp tests, however in the early tests a roughly constant displacement rate was used, and in the computer controlled tests a constant loading rate was used.

During the tests, hysteresis loops of axial load versus diametral displacement were recorded periodically. Also, continuous time records of axial load and diametral displacement were maintained. The strains reported herein are calculated axial strains. The axial elastic strains were calculated from the measured stress range and the modulus for the <001> crystal direction, 7.58×10^4 MPa. The axial inelastic strain was assumed to be twice the diametral inelastic strain based on constancy of volume.

RESULTS

Some results of the 1050 and 1015 °C fatigue and creep-fatigue test results are shown in tables I to III. Shown are the cycle type; cyclic life (N_f); the values for the initial cycles and at half life of the total axial strain range ($\Delta\varepsilon_{tot}$), inelastic axial strain range ($\Delta\varepsilon_{in}$), the individual components of $\Delta\varepsilon_{in}$, stress range ($\Delta\sigma$), and maximum stress (σ_{max}); and the cycle times at N_i, $0.5N_f$, and $0.9N_f$, and average (t_{av}).

Constitutive Behavior

Cyclic stress-strain behavior at half life, $0.5N_f$, for the pp tests is shown in figure 1 for both the 1015 and 1050 °C tests. A cyclic strain hardening exponent of 0.4 fits the data at both temperatures reasonably well. At these high temperatures the effect of temperature on $\Delta\sigma$ is substantial. The estimated 35 °C temperature difference produces about a 150 MPa difference in $\Delta\sigma$ at $\Delta\varepsilon_{in}$ equal to 0.005.

The constitutive behavior of PWA 1480 at 1015 and 1050 °C for all the stress dwell creep-fatigue cycle types studied is characterized by extreme cyclic softening. As a basis for discussion, stress-strain, strain-time, and stress-time plots corresponding to the first cycle, $0.5N_f$, and near failure for a typical cp test at 1050 °C are presented in figure 2. Shown below the three loops are various other measures of the stress-strain-time behavior. This cp test also represents many of the features of the pc and cc tests.

The increase in $\Delta\varepsilon_{in}$ with cycling, which occurred for all cycle types, may be seen for the cp test represented in figure 2. The increase in $\Delta\varepsilon_{in}$ on a percentage basis measured at $0.5N_f$ was roughly independent of

$\Delta\varepsilon_{in}$ and test temperature. At $0.5N_f$, $\Delta\varepsilon_{in}$ had increased an average of approximately 25 percent for the pp tests, approximately 15 percent for the cp and pc tests, but generally less than 5 percent for the cc tests.

For the 1050 °C tests, the decrease in $\Delta\sigma$ at $0.5N_f$ averaged approximately 10 percent for the pp and cp tests, but was slightly higher for the pc tests, approximately 15 percent. In the cc tests $\Delta\sigma$ was, of course, maintained constant. For the cp and pc tests at 1015 °C, the decrease in $\Delta\sigma$ appeared to be smaller than for those tests at 1050 °C, but there is considerable scatter in the data.

The most dramatic change with cycling in the creep-fatigue tests was the increase in creep rates. This is reflected in the cycle times shown in figure 2. At $0.5N_f$, the cycle time has decreased by 77 percent, though $\Delta\varepsilon_{cp}$ has decreased by only 25 percent. In many tests there was no reduction in the amount of creep strain per cycle. Still, by $0.5N_f$ the reduction in cycle time was typically approximately 80 percent in the cp and pc tests, and more than 95 percent in the cc tests. For the 1050 °C tests, by $0.5N_f$ the cycle times were approaching that of the pp tests. However, at 1015 °C creep rates were substantially slower than at 1050 °C, and average cycle times for some of the cp and pc tests with high $\Delta\varepsilon_{in}$ or low creep stress were roughly 100 times longer than that for a pp test.

Though the creep strain per cycle in the creep-fatigue tests typically did not decrease much during cycling on an absolute basis, it did decrease as a fraction of the total inelastic strain range. It may be seen in figure 2 that the fraction of pp strain, f_{pp}, increases with cycling at the expense of f_{cp}. This occurred to a greater degree in the 1050 °C tests than in the 1015 °C tests.

Rounding of the ends of the hysteresis loops where the direction of straining is reversed such as seen at the bottom of the hysteresis loops in figure 2, also occurred in the pp and pc tests at 1050 °C. This effect is due to the rapid creep rates which allows continued straining while the stress is being reduced. This effect was much less evident in the 1015 °C tests.

Another interesting observation in the creep-fatigue tests was that for the same absolute stress level, creep rates were higher in compression than in tension. This effect was observed in comparisons of cp and pc tests, but was most readily seen in the cc tests. Creep rates in compression were about 1.5 to 2 times higher than those in tension.

Life Behavior

For both the fatigue and stress dwell creep-fatigue tests conducted in this study, the life of PWA 1480 has been found to correlate well with a model including both $\Delta\varepsilon_{in}$ and $\Delta\sigma$. This model provides considerably better correlations than those based on $\Delta\varepsilon_{in}$ alone, $\Delta\varepsilon_{in}$ and σ_{max}, or $\Delta\varepsilon_{in}$ and t_{av}.

Table IV shows a summary of the results of regression analyses of the data for all test types at either test temperature using various models. In each case, log N_f has been regressed against the logarithmis of the "independent" variables. That is, power law relationships between the variables have been assumed. These various equations test the basic dependencies of life on

frequency, strain rate, or σ_{max} used in various models including Strain-Range-Partitioning (ref. 4), Frequency-Separation (ref. 5), Frequency-Modified (ref. 6), and Damage-Rate (ref. 7).

The 1050 °C results will be examined first since they are more clear. As previously indicated, care was taken in the design of this series of tests to reduce as much as possible the correlation between the two "independent" variables in the creep-fatigue tests, total strain range and dwell stress. Tests employed various total strain ranges, but only two dwell stress levels (±). For this data set, even with the pp tests included, $\Delta\sigma$ and σ_{max} are only 25 and 16 percent (R-values) correlated with $\Delta\varepsilon_{in}$, respectively.

It may be seen in Table IV that the model $N_f = \alpha\ \Delta\sigma^{\gamma}$ provides a better fit than the single variable models containing $\Delta\varepsilon$, σ_{max}, or t_{av}, or any of the two variable models not including $\Delta\sigma$. Neither the addition of σ_{max} or t_{av} to $\Delta\varepsilon_{in}$ in the model provides substantial improvement. The model $N_f = \alpha\ \Delta\varepsilon_{in}^{\beta}\ \Delta\sigma^{\gamma}$ provides the best fit of all. Note also that in the models containing σ_{max} or t_{av} together with $\Delta\varepsilon$, the absolute values of the T-ratios for their coefficients are much less than 3, the usually accepted value for statistical significance. A visual example of the significance of $\Delta\sigma$ in the model is shown in figure 3. Plots of $N_{f,obs}$ and $N_{f,pred}$ are shown for the two models $N_f = \alpha\ \Delta\varepsilon_{in}^{\beta}$ and $N_f = \alpha\ \Delta\varepsilon_{in}^{\beta}\ \Delta\sigma^{\gamma}$.

Also, the model $N_f = \alpha\ \Delta\varepsilon_{in}^{\beta}\ \Delta\sigma^{\gamma}$ provides the best fit for individual analyses of each cycle type. The best fit coefficients β and γ are not the same for each cycle type, as might be expected. Still, equations using the average values of β and γ, -1.26 and -3.08, provide good fits for the individual cycle types. The values of α in these equations are shown in Table V.

It is well demonstrated by the cc tests that $\Delta\sigma$ is more significant than σ_{max} in determining life. Three tests were conducted with σ_{max} and σ_{min} of about +200/-200 MPa, or a $\Delta\sigma$ of about 400 MPa. An additional cc test at 1050 °C, the first listed in Table V, had about the same σ_{max}, 210 MPa, but a larger $\Delta\sigma$, 474 MPa. The life of this test was reduced to about 1/3 of that expected for a +200/-200 MPa test with the same $\Delta\varepsilon_{in}$. In the fourth test listed in Table V it was intended to increase σ_{max} but keep $\Delta\sigma$ the same as for the first tests. Actually, σ_{max} was increased about 30 percent to 257 MPa, but $\Delta\sigma$ was also increased about 10 percent, and still life increased relative to the +200/-200 MPa tests. For these cc tests alone, R^2 for the model $N_f = \alpha\ \Delta\varepsilon_{in}^{\beta}\ \sigma_{max}^{\gamma}$ is 40 percent, only sightly better than the value of 37 percent for $N_f = \alpha\ \Delta\varepsilon_{in}^{\beta}$, and considerably less than the value of 76 percent for $N_f = \alpha\ \Delta\varepsilon_{in}^{\beta}\ \Delta\sigma^{\gamma}$.

For the tests at 1015 °C, the model containing $\Delta\sigma$ alone provides no better correlation than that containing $\Delta\varepsilon_{in}$, however this could be explained by the high degree of correlation between $\Delta\sigma$ and $\Delta\varepsilon_{in}$ in these tests, R of 80 percent. As indicated previously, the dwell stress levels were increased more or less commensurately with $\Delta\varepsilon_{in}$ among the creep-fatigue tests at 1015 °C in order to reduce test times. Since $\Delta\varepsilon_{in}$ is strongly correlated with $\Delta\sigma$, life correlates equally well with either variable. However, as for the tests at 1050 °C, σ_{max} does not provide a good correlation, nor does t_{av}, and the model $N_f = \alpha\ \Delta\varepsilon_{in}^{\beta}\ \Delta\sigma^{\gamma}$ provides the best correlation. Figure 4 shows a comparison of the predictions of the models $N_f = \alpha\ \Delta\varepsilon_{in}^{\beta}$ and $N_f = \alpha\ \Delta\varepsilon_{in}^{\beta}\ \Delta\sigma^{\gamma}$.

The best fit values of β and γ for the latter model are -1.00 and -2.70. Values of α which provide the best fit for each cycle type are shown in Table V.

It may be seen that correlations using all the models are better for the 1015 °C data than for the 1050 °C data. This is largely because the 1015 °C data cover a greater range of the "independent" variables.

Failure Mode

Internal crack initiation at pores was the predominant failure mode in these tests. For the creep-fatigue tests, in 80 percent of the specimens cracking initiated at many internal pores and linked up before the final overload, as may be seen on the fracture face shown in figure 5. Others appeared to have a dominant crack which initiated near the surface, possibly at a pore, but generally the fracture faces were heavily oxidized and difficult to interpret. Fracture surfaces with this appearance were more common for the pp tests. Still, the majority of pp tests failed at multiple internal pores. It is clear that in these isothermal creep-fatigue tests few, if any, failures initiated in the coating, or at the surface of the superalloy because of a defect in the coating. Of course, the failure mode of bare specimens at these high test temperatures might be quite different.

DISCUSSION

Except in that it permits inelastic strain, creep does not have a great effect on the cyclic life of the coated single crystal superalloy, PWA 1480. On any basis of comparison, and particularly when compared on the basis of $N_f = \alpha\ \Delta\varepsilon^{\beta}\ \Delta\sigma^{\gamma}$ as in Table V, lives for the creep-fatigue cycles are not greatly, if at all, worse than those for the pp tests. Though life may be lower for the cp cycle than for the others, it is only about 30 percent lower than the average for the other cycles. Lives for the other cycles may all be the same.

In fact, there appears to be no time dependent process having a great effect on life. This is shown by the lack of any substantial improvement when t_{av} is included in the life models. Neither creep nor the environmental degradation have affected the coated single crystal superalloy. The mechanisms of creep degradation in polycrystalline alloys such as grain boundary cavitation or sliding obviously cannot occur, and the environment cannot affect the internal crack propagation mode of failure.

The successful life model containing $\Delta\varepsilon_{in}$ and $\Delta\sigma$ is unusual, and may be peculiar to the coated single crystal superalloy system studied. Crack initiation in high temperature creep-fatigue, at least for polycrystalline materials, is usually found to be determined by $\Delta\varepsilon_{in}$ and some measure of time dependent damage processes such as creep cavitation at grain boundaries or oxidation attack. For instance, frequency or strain rate is introduced into the model (refs. 5 to 7). Or, in the Strain-range-Partitioning Model (ref. 4), more or less damage may be assigned to the inelastic strain produced by, say, a cycle with creep in tension than that produced by the rapid straining in a "pure" fatigue cycle.

The internal crack initiation observed and the importance of $\Delta\sigma$ in the life model may reflect that crack propagation is a significant portion of life in these tests. Since the cracks are protected from the atmosphere, it might be expected the crack growth rates are relatively low, and while crack initiation is thought to be primarily driven by $\Delta\varepsilon_{in}$, $\Delta\sigma$ can be tied to crack propagation rates.

Elber (ref. 8) introduced the concept that a crack may not close when the stress intensity, K, is zero, but at some positive K. The effective ΔK driving crack growth, ΔK_{eff}, is taken as $K_{max}-K_{cl}$, where K_{cl} is the K at which closure occurs. It has been shown that compressive overloads increase subsequent fatigue crack growth rates and that the increase is greater with both increasing peak stress and frequency of the compressive overloads (refs. 9 to 11). Such effects have been explained on the basis of reduced K_{cl}, which increases ΔK_{eff}. It has been proposed that compression may flatten roughness of the crack faces and reduce thus K_{cl}. Reversed plasticity may also reduce the size of the plastic zone ahead of a crack, again reducing the K_{cl}. Thus, for reversed tension-compression tests such as conducted herein, ΔK_{eff} is expected to be more directly related to $\Delta\sigma$ than to σ_{max} through the effect of compressive loading in reducing K_{cl}.

These concepts offer a basis for understanding the present results, still some caution is necessary. The studies cited on the effects of compressive overloads, and the models to explain them, apply strictly to linear elastic conditions and "long" cracks. In the present tests, general yielding occurs. Also, if crack growth does indeed constitute a major portion of life, then it would appear that for much of that time the growing cracks might be described as "short". Still speaking of the linear elastic situation, closure of the crack faces at $K > 0$ occurs behind the crack tip in its plastic wake. Since "short" cracks would not have great length of wake behind them, K_{cl} should be near zero and thus ΔK_{eff} would not be expected to be greatly affected by additional reduction of K_{cl} (ref. 12). Still, the results on this particular material clearly show that cyclic life is reduced by increasing the magnitude of the compressive stress in the cycle, and closure effects on crack growth rates may well offer the explanation.

RESULTS AND CONCLUSIONS

Fatigue tests at 0.1 Hz and cp, pc, and cc type creep-fatigue tests have been conducted on NiCoCrAlY coated specimens of a single crystal superalloy, PWA 1480, at 1050 °C and about 1015 °C. The following results and conclusions were obtained.

1. Considerable cyclic softening occurred for all test cycles, evidenced particularly by rapidly increasing creep rates in the creep-fatigue tests.

2. Lives for the pp, cp, pc, and cc cycles were not greatly different, however those for the cp cycle did appear to be lowest at both test temperatures.

3. A life model, $N_f = \alpha\ \Delta\varepsilon_{in}^{\ \beta}\ \Delta\sigma^{\gamma}$, was found to provide good correlation for all cycle types, better than models based on $\Delta\varepsilon_{in}$ alone, or $\Delta\varepsilon_{in}$ with either σ_{max} or t_{av}.

4. For all test types, failure occurred predominately by multiple internal cracking originating at porosity.

5. The strong correlation of life with $\Delta\sigma$ may reflect a significant crack growth period in the life of the specimens.

6. The lack of improvement in the models when average cycle time was considered appears to reflect that neither is there a large effect of strain rate on the damage mechanisms in the single crystal material, nor any environmental effect due to the internal cracking mode of failure.

REFERENCES

1. Gell M., Duhl D.N., and Giamei A.F., in Superalloys 1980, American Society for Metals, Metals Park, Ohio, 1980, pp. 205-214.

2. Shah D.M., and Duhl D.N., in Superalloys 1984, Metallurgical Society of AIME, Warrendale, Pennsylvania, 1984, pp. 105-114.

3. Hirschberg, M.H., in Manual on Low Cycle Fatigue Testing, ASTM STP 465, American Society for Testing and Materials, Philadelphia, 1969, pp. 67-86.

4. Manson S.S., Halford G.R., and Hirschberg M.H., in Symposium on Design for Elevated Temperature Environment, American Society of Mechanical Engineers, New York, 1971, pp. 12-24.

5. Coffin L.F., in 1976 ASME-MPC Symposium on Creep-Fatigue Interaction, MPC3, Amercian Society of Mechanical Engineers, New York, pp. 349-363.

6. Ostergren W.J., in 1976 ASME-MPC Symposium on Creep-Fatigue Interaction, MPC3, American Society of Mechanical Engineers, New York, pp. 179-202.

7. Majumdar S., and Maiya, P.S., in 1976 ASME-MPC Symposium on Creep-Fatigue Interaction, MPC3, American Society of Mechanical Engineers, New York, pp. 323-335.

8. Elber W., in Damage Tolerance in Aircraft Structures, American Society for Testing and Materials, STP 486, Philadelphia, 1971, pp. 230-242.

9. Au P., Topper T.H., and El Haddad M.L., in Behavior of Short Cracks in Airfrace Components, AGARD Conf. Proc. No. 328 NATO Advisory Group for Aerospace Research and Development, France, 1983, pp. 11.1-11.7.

10. Yu M.T., Topper T.H., and Au P., Fatigue '84, ed. C.J. Beevers, Engineering Materials Advisory Services, Warley, UK, Vol. 1, 1984, p. 79.

11. Zaiken E., and Ritchie R.O., Engineering Fracture Mechanics, Vol. 22, No. 1, 1985, pp. 35-48.

12. Suresh S. and Ritchie R.O., International Metals Reviews, Vol. 29, No. 6, 1984, pp. 445-476.

TABLE I. - LOW CYCLE FATIGUE DATA

Cycle type	Specimen number	Life, cycles	$\Delta\varepsilon_{in}$, percent		$\Delta\varepsilon_{tot}$, percent	$\Delta\sigma$, MPa		σ_{max}, MPa		σ_{min}, MPa	
			N1	0.5 N_f		N1	0.5 N_f	N1	0.5 N_f	N1	0.5 N_f
1050 °C											
pp	240	110	0.76	0.92	1.86	780	766	390	388	-391	-378
	60	580	.36	.47	1.29	697	681	348	331	-350	-300
	77	900	.43	.52	1.26	623	571	319	292	-303	-279
	38	950	.27	.32	1.05	591	553	292	275	-299	-278
	261	1000	.38	.47	1.16	584	537	285	274	-299	-263
	23	2900	.19	.30	.87	531	416	270	210	-261	-206
cp	87	85	1.12	1.20	2.04	678	655	255	255	-423	-400
	224	160	0.72	0.82	1.50	587	528	197	197	-390	-331
	262	300	.72	.810	1.53	608	559	246	163	-362	-313
	228	350	.83	.89	1.50	504	454	201	201	-303	-253
	66	400	.64	.69	1.30	498	465	205	205	-292	-260
	256	810	.57	.60	1.27	539	505	201	201	-338	-304
	260	1150	.46	.52	1.12	500	438	201	201	-299	-237
pc	92	134	0.71	0.85	1.62	654	625	405	376	-248	-248
	91	610	.69	.81	1.62	658	639	399	379	-260	-260
	206	930	.65	.76	1.42	582	592	378	287	-204	-205
	180	1250	.82	.910	1.68	598	490	403	292	-196	-194
	245	1410	.79	.90	1.54	566	469	365	266	-201	-203
	235	1700	.44	.52	1.12	513	445	312	247	-201	-199
	241	1650	.64	.71	1.30	533	419	338	225	-195	-194
cc	244	370	0.68	0.70	1.32	474	474	210	210	-263	-263
	192	790	.87	.87	1.41	412	412	206	206	-206	-205
	170	990	.65	.68	1.20	403	403	205	205	-197	-197
	172	1100	.70	.74	1.30	442	439	260	257	-182	-182
	189	2110	.20	.30	.90	400	400	199	199	-201	-201
1015 °C											
pp	84	174	0.55	0.62	1.80	945	904	478	457	-467	-447
	49	192	.70	.81	2.02	983	941	505	478	-478	-463
	184	2021	.31	.38	1.08	603	521	312	275	-291	-239
	159	2314	.12	.15	0.85	557	529	279	276	-279	-252
	257	3900	.14	.16	.77	503	439	255	227	-248	-212
	182	7870	.03	.05	.05	374	344	187	166	-187	-177
cp	191	15	1.80	1.95	3.32	1104	1091	428	429	-676	-663
	187	78	0.68	1.16	1.85	758	803	260	270	-498	-533
	186	146	.25	0.40	1.18	623	681	208	206	-416	-473
	173	218	.70	.58	1.51	680	644	208	208	-473	-436
	176	610	.15	.30	0.90	551	531	332	345	-218	-186
pc	164	29	1.32	1.37	2.44	831	826	572	569	-260	-260
	18	54	0.88	0.88	2.01	862	856	499	494	-260	-260
	44	340	.49	.62	1.43	691	603	483	396	-208	-208
	95	730	.27	.34	1.10	665	613	359	395	-237	-218
	190	2101	.20	.30	0.90	523	467	330	276	-192	-192
cc	171	192	0.92	0.98	1.63	514	514	257	257	-257	-257
	154	724	.71	.72	1.37	499	499	250	250	-250	-250
	179	1826	.20	.30	0.88	519	436	270	218	-250	-218

TABLE II. - COMPONENTS OF INELASTIC STRAIN FOR LOW CYCLE FATIGUE TESTS

Cycle type	Specimen number	Life, cycles	$\Delta\varepsilon_{pp}$, percent		$\Delta\varepsilon_{cp}$, percent		$\Delta\varepsilon_{pc}$, percent		$\Delta\varepsilon_{cc}$, percent	
			N1	0.5 N_f	N1	0.5 N_f	N1	0.5 N_f	N1	0.5 N_f
1050 °C										
pp	240	110	0.76	0.92	----	----	----	----	----	----
	60	580	.36	.47	----	----	----	----	----	----
	77	900	.43	.52	----	----	----	----	----	----
	38	950	.27	.32	----	----	----	----	----	----
	261	1000	.38	.47	----	----	----	----	----	----
	23	2900	.19	.30	----	----	----	----	----	----
cp	87	85	0.43	0.52	0.69	0.68	----	----	----	----
	224	160	.29	.46	.28	.23	----	----	----	----
	262	300	.35	.47	.37	.34	----	----	----	----
	228	350	.47	.52	.36	.37	----	----	----	----
	66	440	.36	.46	.43	.36	----	----	----	----
	256	810	.27	.35	.30	.25	----	----	----	----
	260	1150	.23	.3?	.23	15	----	----	----	----
pc	92	195	0.32	0.42	----	----	0.39	0.43	----	----
	91	610	.34	.49	----	----	.35	.32	----	----
	206	930	.28	.38	----	----	.37	.36	----	----
	180	1250	.34	.43	----	----	.48	.48	----	----
	245	1410	.310	.520	----	----	.48	.38	----	----
	241	1650	.29	.52	----	----	.35	.19	----	----
	235	1700	.25	.36	----	----	.19	.16	----	----
cc	244	370	0.23	0.36	0.03	0.07	----	----	0.03	0.07
	192	790	.19	.60	----	----	----	----	.68	.27
	170	990	.17	.43	----	----	----	----	.48	.25
	172	1100	.16	.32	----	----	0.04	0.21	.50	.21
	189	2100	.15	.34	----	---	----	----	.33	.15
1015 °C										
pp	84	174	0.55	0.62	----	----	----	----	----	----
	49	192	.70	.81	----	----	----	----	----	----
	184	2021	.31	.36	----	----	----	----	----	----
	159	2314	.12	.15	----	----	----	----	----	----
	257	3300	.14	.16	----	----	----	----	----	----
	182	7870	.03	.05	----	----	----	----	----	----
cp	191	15	0.80	0.82	1.00	1.14	----	----	----	----
	187	78	.23	.58	0.45	0.58	----	----	----	----
	186	146	.05	.18	.20	.22	----	----	----	----
	173	218	.24	.23	.46	.35	----	----	----	----
	176	610	.11	.20	.05	.12	----	----	----	----
pc	164	29	0.52	0.57	----	----	0.80	0.80	----	----
	18	54	.44	.26	----	----	.44	.62	----	----
	44	340	.090	.25	----	----	.40	.57	----	----
	95	730	.18	.16	----	----	.09	.18	----	----
	190	2101	.11	.12	----	----	.09	.18	----	----
cc	171	192	0.51	0.52	----	----	----	----	0.42	0.46
	154	724	.35	.37	----	----	----	----	.35	.35
	179	1826	.11	.12	----	----	----	----	.09	.18

TABLE III. - CYCLE TIMES FOR LOW CYCLE FATIGUE TESTS

Cycle type	Specimen number	Life, cycles	Time per cycle, min			
			N1	0.5 N_f	0.9 N_f	Average
1050 °C						
pp	240	110	-----	-----	-----	0.17
	60	580	-----	-----	-----	
	77	900	-----	-----	-----	
	38	950	-----	-----	-----	
	261	1000	-----	-----	-----	
	23	2900	-----	-----	-----	
cp	87	85	3.50	1.10	0.50	1.14
	224	160	5.70	.92	.42	1.28
	262	300	0.92	.33	.22	.39
	228	350	.92	.30	.30	.54
	66	440	1.10	.25	.17	.31
	256	810	4.30	.42	.13	.50
	260	1150	2.20	.23	.30	.40
pc	92	195	1.20	0.58	0.50	0.60
	91	610	1.20	.52	.37	.50
	206	930	5.00	.53	.28	.63
	180	1250	5.20	.32	.30	.60
	245	1410	4.50	.27	.20	.40
	241	1650	3.20	.30	.23	.40
	235	1700	1.10	.18	.18	.24
cc	244	370	7.00	0.22	0.20	0.78
	192	790	20.00	.37	.37	.64
	170	990	12.00	.25	.18	.49
	172	1100	40.00	.22	.20	1.45
	189	2110	7.30	.18	.18	.30
1015 °C						
pp	84	174	-----	-----	-----	0.14
	49	192	-----	-----	-----	.16
	184	2021	-----	-----	-----	.15
	159	2314	-----	-----	-----	.15
	257	3900	-----	-----	-----	.12
	182	7870	-----	-----	-----	.15
cp	191	15	-----	-----	-----	15.33
	187	78	18.00	10.00	1.00	4.87
	186	146	14.00	3.00	0.40	4.64
	173	218	37.50	10.00	-----	2.37
	176	610	30.00	18.00	10.00	15.03
pc	164	29	65.00	21.00	9.00	22.14
	18	54	45.00	19.00	11.00	14.66
	44	340	48.00	3.00	1.00	3.92
	95	730	4.00	1.00	0.35	1.23
	190	2101	16.00	1.50	.40	1.20
cc	171	192	9.50	2.50	0.25	7.38
	154	724	0.50	0.25	.12	0.45
	179	1826	5.50	.25	.13	.59

TABLE IV. - COEFFICIENTS FOR MODELS RELATING $\log N_f$ TO THE LOG OF VARIOUS SINGLE VARIABLES AND COMBINATIONS OF $\log \Delta\varepsilon_{in}$ WITH THE LOG OF VARIOUS OTHER VARIABLES, T-RATIOS OF THE COEFFICIENTS, AND THE STANDARD DEVIATIONS AND R^2 VALUES FOR THE REGRESSIONS

Temperature, °C	Constant		Variable								s	R^2, percent
			$\log \Delta\varepsilon_{in}$		$\log \Delta\sigma$		$\log \sigma_{max}$		$\log t_{av}$			
	a	T	Coef.	T	Coef.	T	Coef.	T	Coef.	T		
1050	-0.79	-0.8	-1.66	-3.7	-----	----	-----	----	-----	----	0.32	37
	12.77	6.1	-----	----	-3.68	-4.8	-----	----	-----	----	.29	50
	5.60	2.8	-----	----	-----	----	-1.16	-1.4	-----	----	.39	8
	3.04	22.8	-----	----	-----	----	-----	----	-0.47	-1.7	.38	12
	8.40	4.2	-1.26	-3.8	-3.08	-4.9	-----	----	-----	----	0.23	70
	1.22	0.6	-1.58	-3.5	-----	----	-0.76	-1.1	-----	----	.32	40
	-1.30	-1.1	-1.93	-3.1	-----	----	-----	----	0.20	0.6	.33	38
1015	-1.50	-3.1	-1.76	-8.5	-----	----	-----	----	-----	----	0.34	81
	16.43	9.8	-----	----	-4.96	-8.2	-----	----	-----	----	.33	80
	10.29	4.5	-----	----	-----	----	-3.09	-3.4	-----	----	.60	40
	2.69	21.7	-----	----	-----	----	-----	----	-0.65	-4.3	.53	52
	7.78	3.0	-1.00	-3.8	-2.70	-3.6	-----	----	-----	----	0.26	90
	0.42	0.2	-1.61	-6.1	-----	----	-0.63	-1.0	-----	----	.34	82
	-0.71	-1.4	-1.43	-6.2	-----	----	-----	----	-0.25	-2.3	.30	86

TABLE V. - BEST FIT VALUES OF THE CONSTANT a IN THE LIFE MODELS FOR PWA 1480 SINGLE CRYSTALS AT 1050 and 1015 °C

Cycle type	a	95 percent confidence limits on $a \times 10^{-8}$
1050 °C: $N_f = a\,\Delta\varepsilon^{-1.26}\,\Delta\sigma^{-3.08}$		
pp	2.25x10-8	1.8 to 2.9
cp	1.41	1.0 to 2.0
pc	3.66	2.4 to 5.5
cc	1.86	1.2 to 2.9
1015 °C: $N_f = a\,\Delta\varepsilon^{-1.00}\,\Delta\sigma^{-2.70}$		
pp	0.489x10-8	0.24 to 0.98
cp	.236	.16 to .35
pc	.318	.17 to .60
cc	.360	.11 to 1.18

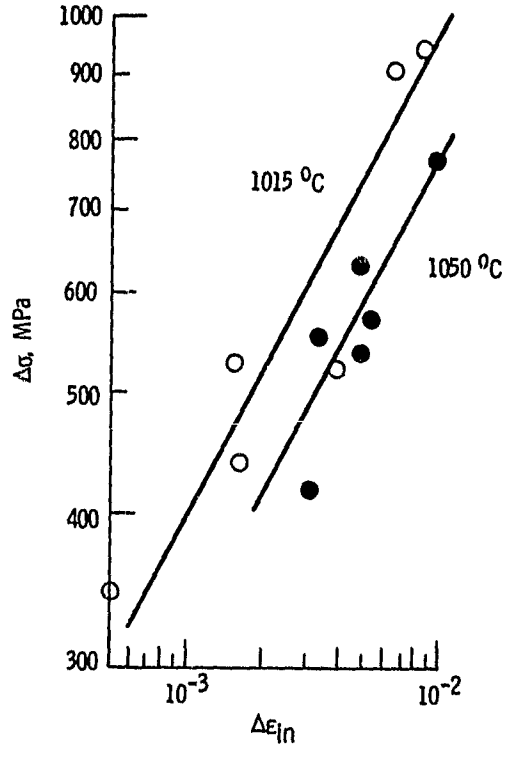

Figure 1. - Cyclic stress-strain behavior of PWA 1480 single crystals in pp cycles at half life.

CS-85-2387

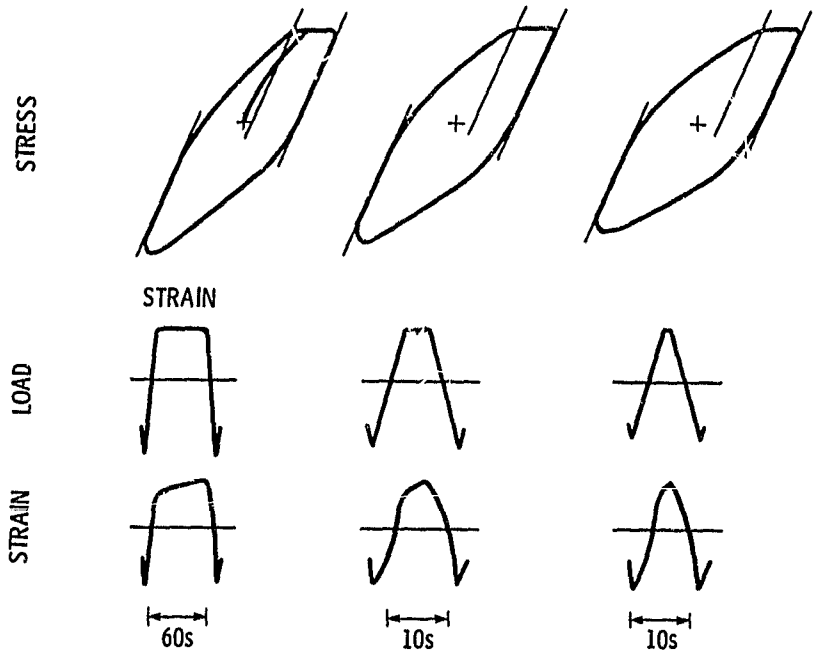

N:	1	210	390
N/N_f:	-	.5	.9
$\Delta\varepsilon_{in}$, %:	.64	.69	.75
$\Delta\sigma$, MPa	490	470	445
f_{pp}:	.56	.65	.68
t_{HOLD}, s:	55	4	1

Figure 2. - Stress-strain-time behavior of a PWA 1480 single crystal in a cp test illustrating typical cyclic softening behavior.

CS-85-2388

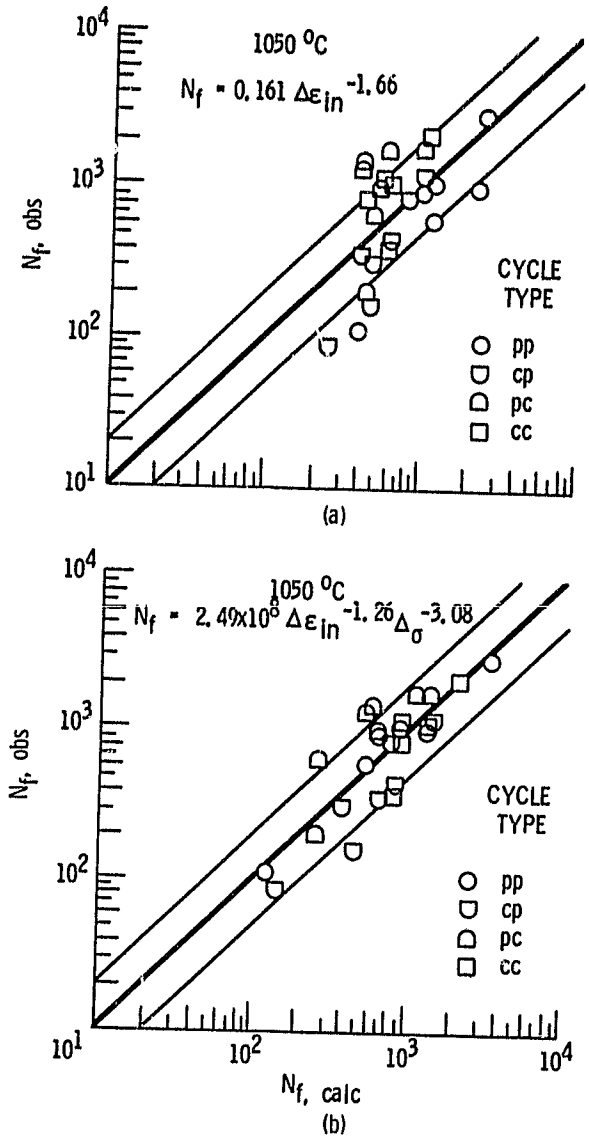

Figure 3. - Observed vs calculated cyclic life of coated PWA 1480 single crystals for various cycle types at 1050 °C: (a) for life model containing only $\Delta\varepsilon_{in}$, and (b) for life model containing both $\Delta\varepsilon_{in}$ and $\Delta\sigma$.

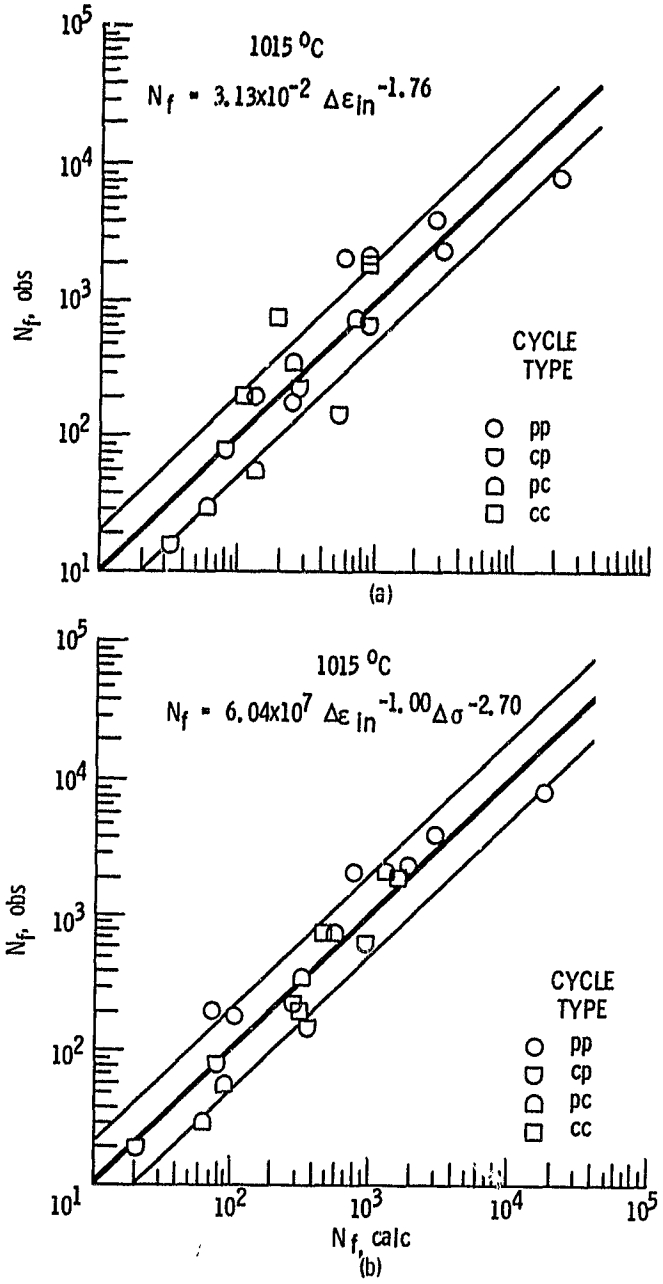

Figure 4. - Observed vs calculated cyclic life of coated PWA 1480 single crystals for various cycle types at 1015 °C: (a) for life model containing only $\Delta\varepsilon_{in}$, and (b) for life model containing both $\Delta\varepsilon_{in}$ and $\Delta\sigma$.

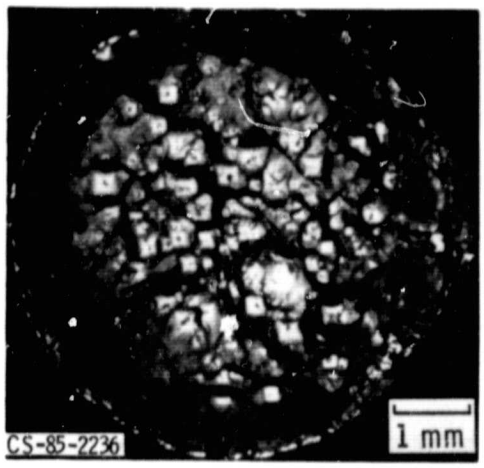

(a) Optical photomicrograph of fracture face.

(b) SEM photomicrograph of a single crack initiation site.

Figure 5. - Multiple internal crack initiation in coated PWA 1480 single crystal low cycle fatigue test specimens.

1. Report No.	2. Government Accession No.	3. Recipient's Catalog No.
NASA TM-87110		

4. Title and Subtitle	5. Report Date
Creep-Fatigue Behavior of NiCoCrAlY Coated PWA 1480 Superalloy Single Crystals	6. Performing Organization Code: 505-33-1A

7. Author(s)	8. Performing Organization Report No.
Robert V. Miner, John Gayda, and Mohan G. Hebsur	E-2710
	10. Work Unit No.

9. Performing Organization Name and Address	11. Contract or Grant No.
National Aeronautics and Space Administration Lewis Research Center Cleveland, Ohio 44135	13. Type of Report and Period Covered: Technical Memorandum

12. Sponsoring Agency Name and Address	14. Sponsoring Agency Code
National Aeronautics and Space Administration Washington, D.C. 20546	

15. Supplementary Notes

Mohan G. Hebsur, NRC-NASA Research Associate.
Prepared for the Symposium on Low-Cycle Fatigue Directions for the Future, sponsored by the American Society for Testing and Materials, Bolton Landing, New York, September 30-October 4, 1985.

16. Abstract

Single crystal specimens of a Ni-base superalloy, PWA 1480, with a low pressure plasma sprayed NiCoCrAlY coating were tested in various 0.1 Hz fatigue and creep-fatigue cycles both at 1015 and 1050 °C. Creep-fatigue tests of the cp, pc, and cc types were conducted with various constant total strain ranges employing creep dwells at various constant stresses. Considerable cyclic softening occurred as was evidenced particularly by rapidly increasing creep rates in the creep-fatigue tests. The cycle time in the creep-fatigue tests typically decreased by more than 80 percent at 0.5 N_f. Though cyclic life did correlate with $\Delta\epsilon_{in}$, a better correlation existed with $\Delta\sigma$ for both the fatigue and creep-fatigue tests, and poor correlations were observed with either σ_{max} or the average cycle time. A model containing both $\Delta\sigma$ and $\Delta\epsilon_{in}$, $N_f = \alpha\,\Delta\epsilon_{in}^{\beta}\,\Delta\sigma^{\gamma}$, with best fit values of α for each cycle type, but the same values of β and γ, was found to provide good correlations. Life lines were not greatly different among the cycle types, differing only by a factor of about three. The cp cycle life line was lowest for both test temperatures, however among the other three cycle types there was no consistent ranking. For all test types failure occurred predominately by multiple internal cracking originating at pores. The strong correlation of life with $\Delta\sigma$ may reflect a significant crack growth period in the life of the specimens. The lack of improvement in the models when average cycle time was considered reflects that neither is there a large effect of strain rate on the damage mechanisms in the single crystal material, nor any environmental effect due to the internal cracking mode of failure.

17. Key Words (Suggested by Author(s))	18. Distribution Statement
Superalloys Fatigue	Unclassified - unlimited STAR Category 26

19. Security Classif. (of this report)	20. Security Classif. (of this page)	21. No. of pages	22. Price*
Unclassified	Unclassified		

*For sale by the National Technical Information Service, Springfield, Virginia 22161